INTERNATIONAL JOURNAL OF PRECISION ENGINEERING AND MANUFACTURING Vol. 14, No. 11, pp. 1989-1996 NOVEMBER 2013 / 1989
DOI: 10.1007/s12541-013-0270-0

Optimal Conditions of SU-8 Mask for Micro-Abrasive Jet Machining of 3-D Freeform Brittle Materials

Jean Bosco Byiringiro[1], Tae Jo Ko[1,#], Ho-Chan Kim[2], and In Hwan Lee[3]

1 School of Mechanical Engineering, Yeungnam University, 214-1 Dae-dong, Gyoungsan, Kyoungbuk 712-749, South Korea
2 Department of Mechanical and Automotive Engineering, Andong National University, 388 Songcheon-dong, Andong, Kyoungbuk, South Korea
3 School of Mechanical Engineering, Chungbuk National University, 12 Gaesin-dong, Cheong-Ju, Chungbuk, South Korea
Corresponding author. E-mail: tjko@yu.ac.kr, Tel: +82-53-810-2576, Fax: +82-53-810-4627

KEYWORDS: Mask hardness, Surface profile of the mask, SU-8 photoresist, 3-D freeform brittle materials

Micro-abrasive jet machining (AJM), also called micro-blasting, is a mainstream machining process that uses abrasive particles for difficult-to-cut workpieces such as glass, carbides, and ceramics. During the micro-blasting process, non-machined areas are covered by a protective mask. Today, either mask fabrication practice or micro-blasting process is well suited and optimized for producing micro-features on planar workpieces. However, the demand for micro-features on three-dimensional (3-D) freeform substrates in micro electro-mechanical systems (MEMS) and lab-on-a-chip devices requires more refined non-planar micro-manufacturing techniques. We focused on devising an appropriate photoresist mask required by micro-AJM processes on the surface of a 3-D freeform workpiece. Fundamental erosion mechanisms based on SU-8 mask properties (hardness, surface roughness, and thickness) were investigated. The optimal conditions were found at an ultraviolet (UV) energy of 12.0752 μJ/μm, focus ratio of 4.8341, and hard baking time of 8.4974 min. Under these settings, the mask hardness and surface roughness were 25.04 HV and 1.14 μm, respectively. The reliability of the fabricated mask was verified through a micro-AJM process. With existing plant conditions, the engraved micro-feature dimensions on the surface of a 3-D freeform workpiece were 535.3 μm (width) and 11.6 μm (depth).

Manuscript received: February 19, 2013 / Accepted: August 12, 2013

NOMENCLATURE

A = UV energy per unit length (μJ/μm) formed by the ratio of UV power (μW) to scanning speed (μm).
B = Focus ratio (dimensionless) formed by an interaction of the ratio of the focal diameter (μm) to hatch line spacing (μm), and the ratio of Cyclopentanone (C_5H_8O) to SU-8 epoxy resin.
C = Hard baking time (min) at 150°C.

1. Introduction

High quality materials such as carbides, ceramics, composites, semiconductors, glass, diamond, and hardened steel possess high strength and stiffness at elevated temperatures, extreme hardness, high brittleness, a high strength-to-weight ratio, high corrosion and oxidation resistance, and chemical inertness. Although these properties result in superior product performance, their precise shaping and/or machining can be difficult.[1-4] The emergence of advanced engineering materials, stringent design requirements, and intricate shapes and unusual sizes of the workpiece restrict the use of conventional machining methods. For instance, accurate fabrication of three-dimensional (3-D) micro-structures with well-defined curved surface contours is of great importance for various mechanical, optical, and electronic devices and subsystems. Thus, more attention is directed toward machining processes in which the mechanical properties of the workpiece materials do not impose limits on the material removal process.[3-7] In this regard, non-conventional machining techniques come into practice as a possible alternative with respect to machining ability, shape complexity, surface integrity, and miniaturization requirements.

Recently, micro-abrasive jet machining (AJM), a new micro-engraving technology, has established itself among the mainstream machining processes as the method of choice when cutting materials that are difficult to machine by solid cutting tools. Micro-AJM is a manufacturing process that utilizes a high-pressure air stream carrying small particles to impinge the workpiece surface for material removal. The removal

occurs due to the erosive action of the particles striking the surface of the workpiece. To realize efficient blasting with a specified pattern, it is essential to apply masking on the work surface. As the masking restricts the size of the pattern, the methods of masking should be selected carefully. The type of masking is selected by considering the required accuracy, cost, and controllability. Masking methods include photoresist, metallic, and printing methods. A photoresist mask is suitable for processes demanding the highest level of accuracy.[5-7,11-17]

Modeling and fabrication of the photoresist mask structure are key processes in highly accurate micro-blasting. There are a number of commercially available photoresists suitable for high aspect ratio (HAR) applications. SU-8, an epoxy-based negative photoresist, has become the favorite photoresist for HAR and 3-D lithographic patterning due to its excellent coating, planarization, and processing properties as well as its mechanical and chemical stability. However, as feature sizes get smaller and pattern complexity increases, a number of material-related issues need to be carefully considered.[8-17] For instance, after Lee *et al.*[11] compared the SU-8 mask and the Watershed 11110 mask for use in the micro-AJM process; they concluded that the SU-8 photoresist, as a highly sensitive and viscous epoxy resin, can be used for accurate and precise fabrication of a photoresist mask onto a 2-D planar workpiece at reasonable cost. Nevertheless, high viscosity (45,000-80,000 cSt) of the SU-8 photoresist, as determined by the UV range, requires both spin coating and soft-backing processes to acquire uniform thickness for UV illumination.

A few decades ago, micro-stereolithography (SL) was developed as a prototyping method that cures photosensitive resin under ultraviolet (UV) light of the proper wavelength. SL can be used to fabricate 3-D solid parts. After the first micro-SL apparatus appeared, a number of micro-SL devices have been used. They operate with similar principles but vary in the prototyping materials, light sources, and curing processes used, thus resulting in many subfamilies of micro-SL methods.[8,14,15] For instance, Choi *et al.*[8] introduced the micro-SL system using a UV lamp and optical fibers instead of UV laser beam because the UV lamps are reasonably priced compared to UV lasers. Although the developed micro-SL systems demonstrated high performance, previous studies have significantly contributed to the understanding of the initiation of photosensitive resin under UV light.

Micro-mask fabrication processes are well suited and have been optimized for producing micro-features on planar (2-D) workpieces.[10-13] However, the demand for micro-features on 3-D freeform surfaces in micro-electromechanical systems (MEMs) and lab-on-a-chip devices (e.g., micro-lenses and other micro-optical components, and contoured microfluidic channels), requires alternative non-planar micro-manufacturing processes to be developed.

In the a previous publication by the authors,[17] 3-D freeform photoresist masks were devised (without spin coating and soft-baking) and validated through the micro-engraving features on the surfaces of 3-D non-planar workpieces. However, the optimal mask fabrication conditions are needed to be found. The main objective of this study is to develop a mathematical model and determine the optimal conditions for the fabrication of an appropriate 3-D freeform photoresist mask, as required by micro-AJM processes.

2. Experimental Procedure

2.1 Computer-aided design (CAD) modeling of a 3-D freeform mask

At this stage, mathematical (rectangular, circular, and T-channel) and non-mathematical symbol (YU character) micro-features were scaled down to 0.02 inches (around 500 μm) and 10 points (Myriad professional font), respectively. To ensure the accuracy and consistency of the micro-fabrication parameters with a layer-by-layer scheme, the slicing steps in the CAD modeling were set to 100 μm. After slicing, it was necessary to carefully choose the scanning path and tool path strategy by taking into consideration the existing plants (micro-SL and micro-AJM setups with only X-Y-Z linear stages). For mask fabrication, a break segment tool path strategy was chosen because a controllable shutter was provided in the system setup to control the solidification process (ON/OFF of

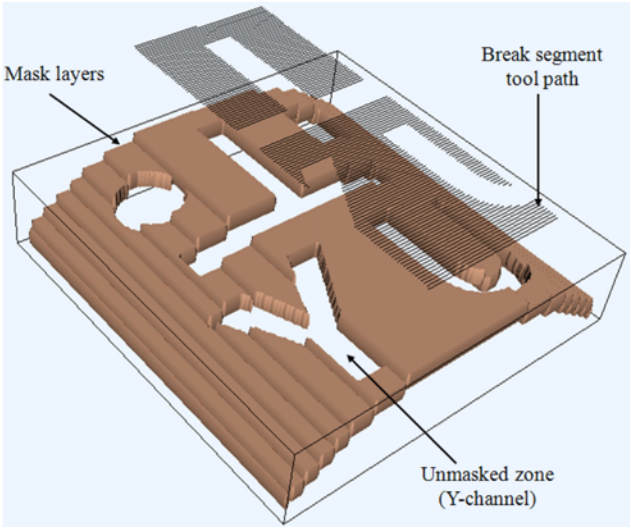

Fig. 1 Layered mask model and break segment tool path strategy

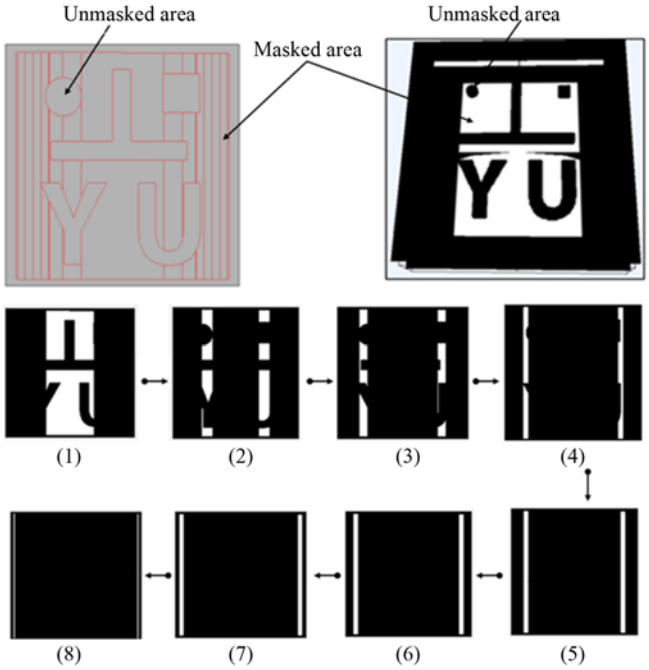

Fig. 2 Layered fabrication scheme from the top (1) to bottom (8)

UV light). Fig. 1 illustrates the 3-D freeform layered mask model and tool path for the first portion of the mask to be created on the surface of the 3-D freeform substrate.

In addition to design complexity, we note that the real implementation of this micro-technology can also be limited by the plant setup; i.e., the degree of freedom. Therefore, in design practice, we correlated the design ideas with practical execution because an actual product often appears some times after the point at which new micro-technologies are ready for practical implementation.

The adopted micro-manufacturing strategy was to start with the top layer and allow the Z-stage to move upward until the bottom layer was reached. Fig. 2 illustrates in detail the overflowing micro-fabrication mask steps (portion-by-portion), starting from the top film as enumerated from (1) to (8).

As mentioned before, for micro-mask fabrication on the surface of a 3-D freeform workpiece, both spin coating and soft baking are not feasible. Therefore, special conditions that may arise on the already scanned portion of the surface due to contact with uncured SU-8 epoxy resin must be considered in the 3-D CAD modeling. The adopted micro-fabrication strategy dictated careful customization of the generated NC code for compatibility with each machine controller. Due to various customizations carried out in the design phase, simulation was considered to be a powerful tool for analyzing the model and exploring processes and checking.

2.2 Resist mask fabrication on 3-D freeform workpiece

All the experiments for SU-8 mask fabrication were conducted by using a developed tunable micro-SL system (Fig. 3) consisting of a commercial spot UV light (INNO-CURE 100N, Lichtzen Co. Ltd.) into which a 100 W high pressure mercury lamp was incorporated to ensure a total UV output energy of 3,000 mW/cm^2.

A liquid light guide (5 mm (f) × 1 m (L)) entered the Newport optical system, which collimated UV light into a microscope objective lens (M-10X, NA=0.25, Newport Corporation, USA). A Patchcord (QMMJ-3S3S-UVVIS 105/125-3-1, NA=0.22, OZ Optics Limited, USA) was used to reduce the beam size and was attached to a 3-axis linear stage (Physik Instrumente, Germany), that was controlled through the LabVIEW program to ensure accurate micro-size displacement.

In the experimental tests, we discovered that an unstable solution (the presence of bubbles) led to the fabrication of defective (slight micro-depressions in the smoothness of a surface) SU-8 photoresist masks. Therefore, after dilution and before exposure, the diluted SU-8 resin was allowed to stabilize in a yellow room for 1 hr. After UV exposure, the workpiece was hard-baked in the oven (OF-02GW, JEIO TECH, Korea) instead of a level plate to ensure micro-mask production with the same conditions. We deliberately manipulated the baking temperature in the range from 65°C to 200°C. It has been found that baking at less than 100°C led to shrinkage and deformation of the SU-8 mask in the development course. Based on our experience, the hard baking process at 150°C inside the oven is more promising for the inexperienced user because, as mentioned in the previous section, in this new fabrication technique onto 3-D freeform workpiece surfaces only one baking process is possible.

After the hard-baking process, the SU-8 resist mask was developed by using SU-8 developer (3 min), which is mainly composed of propylene glycol monomethyl ether acetate (PGMEA). The process was stopped and the mask was rinsed (5 min) by using isopropyl alcohol (IPA). The micro-fabrication approach was considered significant and reasonable because the SU-8 is a negative acting resist. Thus, where the UV light exposes it, the resist becomes insoluble in the developer. In addition, SU-8 is epoxy-based resin, which means that it is very durable and almost impossible to strip.

3. Development of Empirical Models

Based on a previous study by the authors,[17] the most influential SU-8 mask fabrication parameters were combined into a set of three input factors: UV energy, focus ratio, and hard baking time at 150°C.

With a well-defined range of the inputs, the mask hardness and surface profiles were analyzed (micro-Vickers and non-contact profile measurement, respectively) as output responses. Fig. 4 shows surface profiles of the mask (surface roughness and thickness).

In the development of the empirical model, a Box-Behnken design as a response surface methodology was used to further study the quadratic effect of the SU-8 mask fabrication factors. It is believed that for three factors, the Box-Behnken design offers some advantage in requiring fewer runs.[19] In the design settings, 3 mentioned input factors, 1 block, 3 center points, 15 observations, and 2 responses (mask hardness and surface roughness) were set. Table 1 illustrates the factor

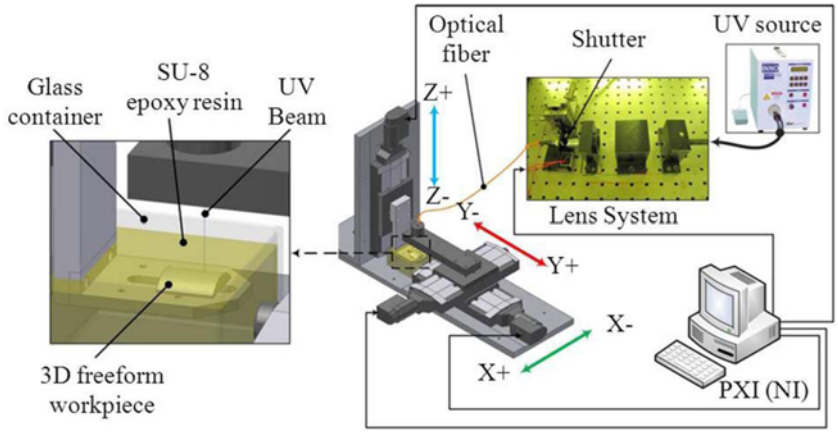

Fig. 3 Developed micro-SL system for micro-mask fabrication

properties for both mask hardness and surface roughness. In our discussion of results, the input factors of UV energy, focus ratio, and hard baking time were termed A, B, and C, respectively, for easy visualization of their interactions. The combinations of UV energy and focus ratio variables are shown in the Eqs. (1) and (2).

$$A = \frac{UV\ Power}{Scanning\ speed} \tag{1}$$

$$B = \frac{Beam\ size}{Hatch\ line\ spacing} \times \frac{Cyclopentanone}{SU-82100} \tag{2}$$

Where; SU-8 2100 is a trade name for the series resists (Chemical name of SU-8 is organic resin solution) and Cyclopentanone (CAS: 120-92-3) is a colorless, water-insoluble liquid obtained from petroleum and used chiefly as a solvent.

After performing the experiment according to the Box-Behnken design approach and recording the results, the data set was entered into the standard folio (Table 2). The data set was analyzed with a risk (significance) level of 0.05, using individual terms. The input variables and output responses in the standard folio were analyzed at high accuracy

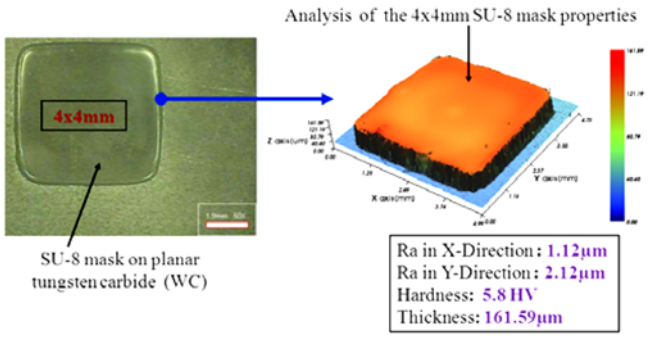

Fig. 4 Analysis of the SU-8 mask properties (100 μm hatch spacing)

Table 1 Factor properties for hardness and surface roughness

Factor	Name	Units	Type	Low	High
A	UV Energy	μJ/μm	Quantitative	7.5	12.5
B	Focus ratio	-	Quantitative	3.5	7.0
C	Baking time	Minutes	Quantitative	7.0	11.0

Table 2 Standard folio for input factors and output responses

S/N	A: UV Energy	B: Focus ratio	C: Hard Baking	Hardness (HV)	Surface roughness (μm)
1	7.5	3.50	9	4.950	0.270
2	7.5	7.00	9	1.120	0.550
3	7.5	5.25	7	1.440	0.250
4	7.5	5.25	11	5.450	0.900
5	10.0	3.50	7	2.520	1.380
6	10.0	7.00	7	5.340	0.570
7	10.0	3.50	11	4.787	1.230
8	10.0	7.00	11	1.690	1.870
9	10.0	5.25	9	5.230	0.820
10	10.0	5.25	9	5.230	0.820
11	10.0	5.25	9	5.230	0.820
12	12.5	3.50	9	5.800	1.010
13	12.5	7.00	9	5.840	0.498
14	12.5	5.25	7	9.900	0.780
15	12.5	5.25	11	1.450	1.050

(R-squared of 96.32% and 99.72% for mask hardness and surface roughness respectively). The Box-Behnken design method advises to utilize P-value displayed in the analysis of variance (ANOVA) tables of results as a reference for the investigation of parameter effects in the empirical model development (the P value is often set to 0.01 or 0.05).

In this study, DOE++ software (version 1.0, ReliaSoft Corporation) was used to evaluate the correlation between input variables and output responses. As shown in the ANOVA (Table 3) for SU-8 mask hardness, the impacts of factors A and C, and interaction factors AC and BC, were more significant because the P-value is less than the risk value.

The P value for B was 0.1159 and interaction factors AB, BB, and CC were 0.0509, 0.088, and 0.1128, respectively, which were close to the risk level (0.05). Therefore, they should also be included in the final empirical model of mask hardness (HV) as shown in the Eq. 3:

$$\begin{aligned} Hardness = {} & -81.3521 + 4.6703A + 4.3503B + 11.4898C + \\ & 0.0139A^2 - 0.2903B^2 - 0.1892C^2 + 0.2211AB - \\ & 0.623AC - 0.4226BC \end{aligned} \tag{3}$$

Moreover, as shown in the ANOVA shown in Table 4 for surface roughness of the SU-8 mask, the effects of factors A, B, and C and their interactions AB, AC, BC, AA, BB, and CC were all significant.

Table 3 ANOVA table for hardness of SU-8 mask

Source of variation	DOF	Sum of squares	Mean squares	F ratio	P-Value
A	1	12.5751	12.5751	21.9475	0.0054
B	1	2.0676	2.0676	3.6085	0.1159
C	1	4.2384	4.2384	7.3974	0.0418
AB	1	3.7442	3.7442	6.5348	0.0509
AC	1	38.8129	38.8129	67.7407	0.0004
BC	1	8.7527	8.7527	15.2762	0.0113
AA	1	0.1556	0.1556	0.2716	0.6245
BB	1	2.5645	2.5645	4.4758	0.0880
CC	1	2.1138	2.1138	3.6892	0.1128
Residual	5	2.8648	0.5730		
Lack of Fit	3	2.8648	0.9549	-	-
Pure Error	2	0.0000	0.0000		
Total	14	77.8896			
Model	9	75.0248	8.3361	14.5491	0.0044

Table 4 ANOVA table for surface roughness of the SU-8 mask

Source of variation	DOF	Sum of squares	Mean squares	F ratio	P-Value
A	1	0.2339	0.2339	164.7148	5.11E-05
B	1	0.0202	0.0202	14.2237	1.3E-02
C	1	0.5356	0.5356	377.1388	6.68E-06
AB	1	0.1568	0.1568	110.4183	1.00E-04
AC	1	0.0361	0.0361	25.4190	4.00E-03
BC	1	0.5256	0.5256	370.1063	7.00E-06
AA	1	0.6256	0.6256	440.5062	4.55E-06
BB	1	0.0504	0.0504	35.4724	1.90E-04
CC	1	0.3384	0.3384	238.2960	2.07E-05
Residual	5	0.0071	0.0014		
Lack of fit	3	0.0071	0.0024	-	-
Pure error	2	0.0000	0.0000		
Total	14	2.5298			
Model	9	2.5227	0.2803	197.3662	7.72E-06

Their P-values were less than the risk level set of 0.05. Therefore, the UV energy (A), focus ratio (B), and hard baking time (C) as well as all their interactions must be included in the final model of the mask surface roughness (Ra), as shown in Eq. (4):

$$Ra = 1.2746 + 1.6858A - 0.9874B - 1.5868C - 0.0604A^2 + 0.0456B^2 + 0.0757C^2 - 0.0453AB - 0.0190AC + 0.1036BC \quad (4)$$

The reliability of the developed empirical models was also supported by the main effects plot for hardness and surface roughness of the SU-8 mask, as shown in Figs. 5 and 6, respectively. From the plots, we observed that the relationships between input factors were very close.

4. Optimization of SU-8 mask Fabrication

The developed empirical models described by Eqs. (3) and (4) were used to optimize the SU-8 micro-mask fabrication parameters. The optimization setting parameters for the input factors were the same as those shown in Table 1, and the response optimization settings are shown in Table 5.

One of the displayed optimal conditions (selected by default) is plotted in Fig. 7. Here, optimal solution 7 was found to be UV energy = 11.8432 μJ/μm, focus ratio = 4.848, and hard baking time = 8.8444 min. Under these settings, the expected mask hardness and surface roughness are 6.3306 HV and 0.7792 μm, respectively. All results for optimal conditions for the SU-8 mask fabrication are shown in the Table 6.

After optimization of the SU-8 micro-mask production, validating experimental work was carried out under optimal settings (Table 6) to confirm the approximated results. As shown in Table 7, the actual results for SU-8 mask hardness were better than the predicted ones (Fig. 8). It has been observed that under optimal settings, the results obtained for SU-8 mask hardness (without spin coating, edge bead removal, and soft baking) were in the same range as the results described in[12,13] through normal lithographic processes.

For the surface roughness of the SU-8 mask, the results obtained under optimal settings correlate well with the predicted ones as shown in Fig. 9. The best optimal condition for SU-8 micro-mask fabrication was found at UV energy = 12.0752 μJ/μm, focus ratio = 4.8341, and hard baking time = 8.4974 min. Under these settings, the mask hardness and surface roughness were found to be 25.04 HV and 1.14 μm, respectively.

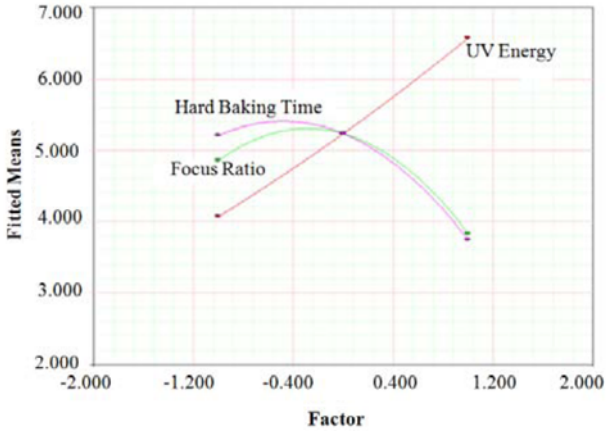

Fig. 5 Main effect plot for mask hardness

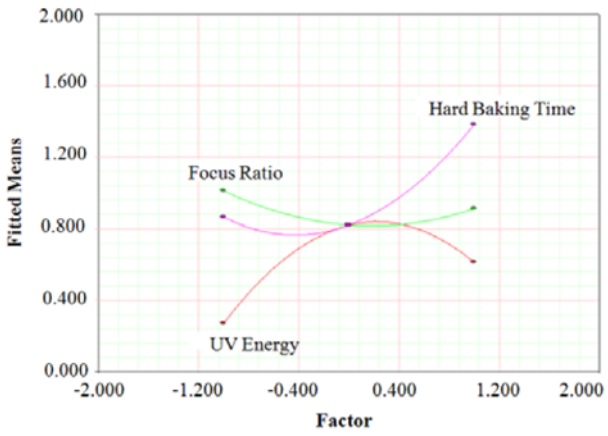

Fig. 6 Main effect plot for surface roughness of the mask

Table 5 Optimization settings for mask properties

Name	Goal	Lower limit	Target	Upper limit
Hardness (HV)	Maximize	1.12	5.23	-
Ra (μm)	Minimize	-	0.82	1.87

Table 6 Optimal conditions for mask required by micro-AJM

Name	UV-Energy	Focus ratio	Baking time	Hardness (HV) (Predicted)	Ra (μm) (Predicted)
Opt. 1	7.5000	4.7056	11.0000	6.5267	0.7825
Opt. 2	8.3623	4.1833	9.6350	5.4385	0.6117
Opt. 3	9.0516	4.2559	9.5830	5.2902	0.7834
Opt. 4	10.0000	7.0000	7.0000	5.2830	0.5910
Opt. 5	10.1778	5.6560	8.4054	5.4871	0.7497
Opt. 6	10.5000	7.0000	7.0000	6.3537	0.5895
Opt. 7	11.8432	4.8948	8.8444	6.3306	0.7792
Opt. 8	12.0495	4.6380	9.3445	5.6091	0.8160
Opt. 9	12.0752	4.8341	8.4974	6.9067	0.7561
Opt. 10	12.0833	7.0000	8.8000	6.2164	0.5735
Opt. 11	12.5000	7.0000	9.0000	6.1404	0.5048
Opt. 12	12.5000	5.2500	7.0000	9.6566	0.7523
Opt. 13	12.5000	6.0331	7.6344	9.3209	0.4487
Opt. 14	12.5000	6.7277	7.1486	10.3893	0.3278

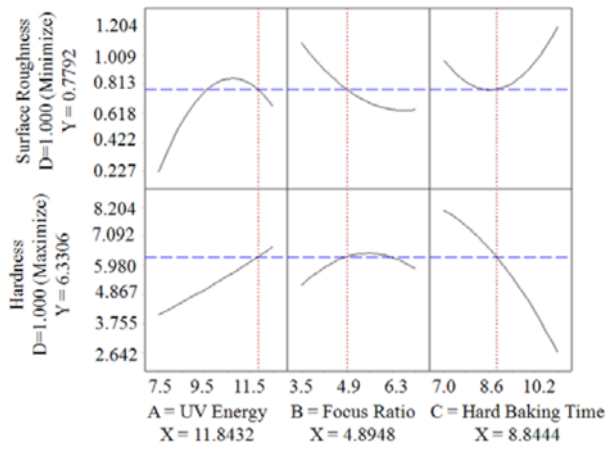

Fig. 7 Plot of predicted optimal solution 7 for SU-8 mask

5. Micro-AJM for Validation of SU-8 Properties

A validating experiment was conducted by using a commercial micro-abrasive sandblaster (Model MV-241 Microblaster, Crystal Mark, Inc., Glendale, CA, USA), into which a mixing device was incorporated to prevent particle bed compaction. An enclosed and vented commercial work chamber (Turbo Station, Crystal Mark, Inc., Glendale, CA USA), into which the nozzle holder and workpiece support were fixed. This is an illuminated work chamber with a built-in dust collector designed for low volume requirements. Dry air at 200 kPa entered the micro-blaster, where it was mixed with aluminum oxide (Al_2O_3) powder with a 17.5 μm nominal diameter, and hardness of 20 GPa. The average velocity of the particles across the jet for a round carbide right angle nozzle with a 457.2 μm inner diameter is around 100 m/s. The micro-blasting conditions are shown in Table 8.

Table 7 Predicted results versus actual results of the SU-8 mask

Name	Hardness (HV) (Predicted)	Hardness (HV) (Actual)	Ra (μm) (Predicted)	Ra (μm) (Actual)
Opt. 1	6.5267	22.92	0.7825	0.820
Opt. 2	5.4385	15.80	0.6117	1.020
Opt. 3	5.2902	21.84	0.7834	0.750
Opt. 4	5.2830	22.20	0.5910	0.138
Opt. 5	5.4871	20.05	0.7497	0.473
Opt. 6	6.3537	19.02	0.5895	0.242
Opt. 7	6.3306	25.86	0.7792	0.650
Opt. 8	5.6091	20.47	0.8160	0.720
Opt. 9	6.9067	25.04	0.7561	1.140
Opt. 10	6.2164	24.42	0.5735	0.580
Opt. 11	6.1404	24.42	0.5048	0.056
Opt. 12	9.6566	24.01	0.7523	0.321
Opt. 13	9.3209	22.71	0.4487	0.459
Opt. 14	10.3893	23.88	0.3278	1.320

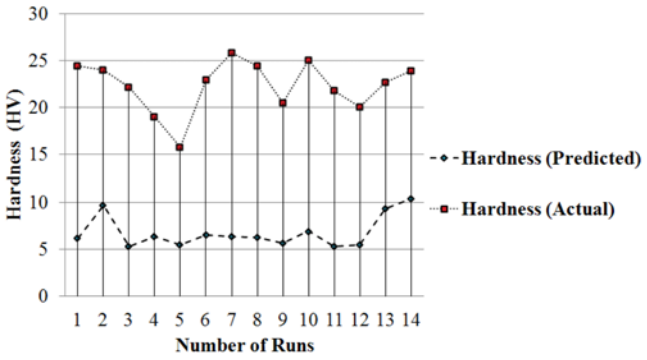

Fig. 8 Predicted versus actual results for mask hardness

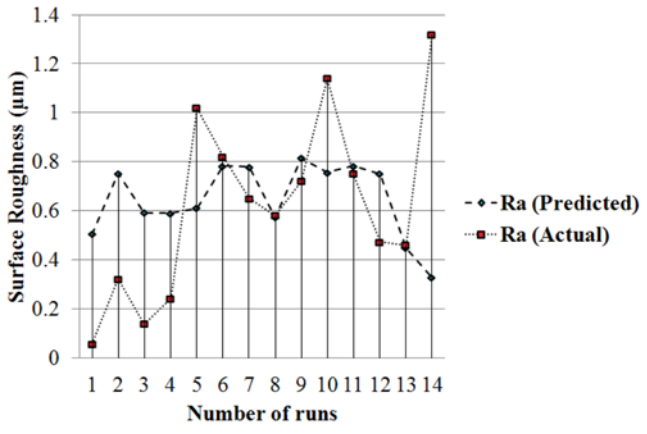

Fig. 9 Predicted versus actual results for surface roughness of mask

For the present results, all blasting conditions remained unchanged during the experimental work. The round right-angle nozzle was used to produce a more uniform particle stream over the mask opening, and reduce possible alignment inaccuracies. The 3-D freeform target was fixed on a rectangular plate, and the nozzle was mounted on a computer-controlled 3-axis linear stage to ensure alignment accuracy as well as position. The tool path strategy[18] was the same as that defined for mask fabrication in the previous section except that instead of having break segments, an overlap scanning strategy was used for micro-blasting at both the masked zone and unmasked zone. The SU-8 photoresist mask consisted of a single film thickness (~160 μm) that was used during the micro-AJM process. Multiple pass machining was performed using alternating forward and backward scans. After micro-AJM, the remaining thin sacrificial SU-8 mask was removed from the main target by using a high temperature of 200°C inside an oven (OF-02GW, JEIO TECH, Korea) for 5 min followed by soaking in a solution of SU-8 (MicroChem, Co. Ltd., USA) developed for 1 hr.

Interestingly, the SU-8 mask was slightly eroded. As indicated in the literature,[5-7] polymeric material (the SU-8 mask) responds in a ductile manner under typical conditions of micro-AJM processes, with the highest erosion rate observed when the particle jet is inclined by 25° to 55° toward the target surface. Brittle material is characterized by a peak in the erosion rate at a normal incidence (90°). As shown in Fig. 10, the insignificant erosion of the SU-8 mask did not affect the final result and can be neglected. Furthermore, even though the photoresist mask was slightly eroded, it remained fully attached to the target. This mask behavior further reinforced the aforementioned hypothesis that a heat effect was not present in this micro-blasting experiment.

The surface roughness and depth (Fig. 10) of the engraved micro-features were analyzed using a Surftest-301 roughness tester (Mitutoyo, MTS Co. Ltd., Japan). As shown in Table 9, the surface roughness (Ra) and the depth were around 1.09 μm and 11.6 μm, respectively. However, it was very problematic to find a highly upright measurement strategy. A microscope was used to measure sizes of the micro-features engraved

Table 8 Micro-AJM conditions for 3-D freeform carbides (WC)

Item	Specification
Target: Tungsten carbide (WC)	25.00×25.00×6.00 (mm)
Micro-abrasives (Al_2O_3)	17.50 μm
Hardness of micro-abrasive	20.00 GPa
Round carbide, right angle nozzle	457.20 μm
Impingement angle	Normal incidence (90°)
Stand-off-distance (SOD)	38.00 mm
Particles velocity (setting=2)	100.00 m/s
Pressure rate	200.00 kPa
Powder mass flow rate	2.62 g/min
Nozzle feed rate	100.00 mm/min
Number of scan	5.00 times
Machining pass	Forward and backward
Hatch lines spacing	100.00 μm
Cutting strategy	Overlap

on surface of the 3-D freeform workpiece.

The micro-features were magnified to estimate the real size, as shown in Fig. 11. Under these experimental conditions, the minimum feature size was measured to be around 535.3 μm.

Conclusion

In the authors' previous work, micro-mask fabrication (micro-SL) and micro-AJM processes were well suited and optimized for producing micro-features on planar workpieces using a variety of materials including carbides, ceramics, composites, semiconductors, a variety of glass, and diamonds. However, the demand for micro-features on 3-D freeform substrates for a variety of industrial applications has compelled the development of superior 3-D non-planar manufacturing techniques. Therefore, there has been a great deal of interest in developing an appropriate photoresist mask that can effectively protect surface of a 3-D freeform target during micro-AJM processes. We developed an empirical model for SU-8 mask fabrication based on the mask properties required by micro-AJM (hardness, surface roughness, and thickness), and optimized the SU-8 mask fabrication conditions. Furthermore, the fabricated SU-8 mask was successfully tested and verified through micro-blasting experiments. With these experimental conditions, the achieved feature size on the surface of a 3-D freeform workpiece was around 535.3 μm in width and 11.6 μm in depth. Based on these results, the fabricated SU-8 mask was considered to be reliable.

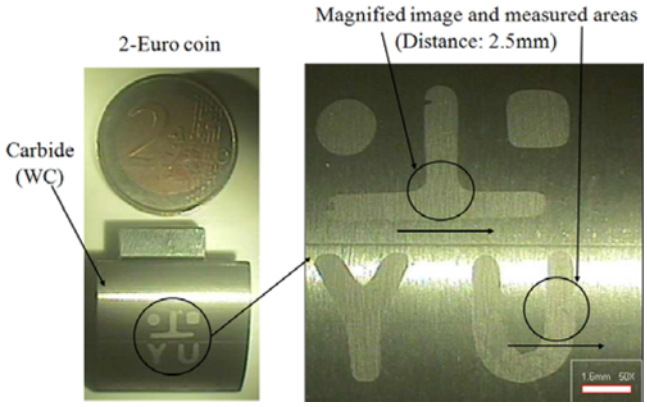

Fig. 10 Mathematical and non-mathematical features on 3-D freeform carbides (WC)

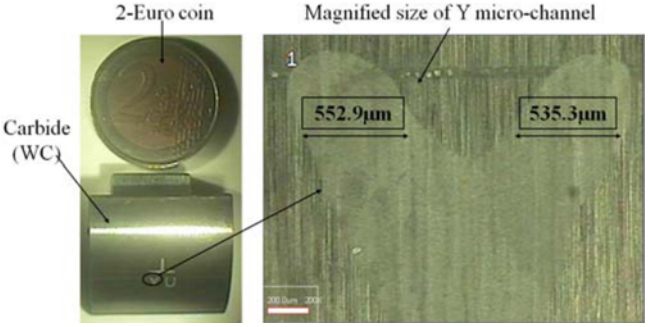

Fig. 11 Y-Channel on surface of 3-D freeform carbide (WC)

ACKNOWLEDGEMENT

This work was supported by the Basic Science Research Program through the National Research Program of the National Research Foundation of Korea (NRF), funded by Ministry of Education, Science and Technology (MEST) of Korean government (grant no. 2011-0013496).

REFERENCES

1. Masuzawa, T., "State of the art of micromachining," CIRP Annals - Manufacturing Technology, Vol. 49, No. 2, pp. 473-488, 2000.
2. Jain, N. K. and Jain, V. K., "Modeling of material removal in mechanical type advanced machining processes: A state-of-art review," International Journal of Machine Tools and Manufacture, Vol. 41, No. 11, pp. 1573-1635, 2001.
3. Slikkerveer, P. J., Bouten, P. C. P., and de Haas, F. C. M., "High quality mechanical etching of brittle materials by powder blasting," Sensors and Actuators A: Physical, Vol. 85, No. 1-3, pp. 296-303, 2000.
4. Wakuda, M., Yamauchi, Y., and Kanzaki, S., "Effect of workpiece properties on machinability in abrasive jet machining of ceramic materials," Precision Engineering, Vol. 26, No. 2, pp. 193-198, 2002.
5. Getu, H., Ghobeity, A., Spelt, J. K., and Papini, M., "Abrasive jet micromachining of polymethylmethacrylate," Wear, Vol. 263, No. 7-12, pp. 1008-1015, 2007.
6. Getu, H., Ghobeity, A., Spelt, J. K., and Papini, M., "Abrasive jet micromachining of acrylic and polycarbonate polymers at oblique angles of attack," Wear, Vol. 265, No. 5-6, pp. 888-901, 2008.
7. Burzynski, T. and Papini, M., "Level set methods for the modelling of surface evolution in the abrasive jet micromachining of features used in MEMS and microfluidic devices," Journal of Micromechanics and Microengineering, Vol. 20, No. 8, pp. 085004, 2010.
8. Choi, J., Kang, H. W., Lee, I., Ko, T. J., and Cho, D. W., "Development of micro-stereolithography technology using a uv lamp and optical fiber," The International Journal of Advanced Manufacturing Technology, Vol. 41, No. 3-4, pp. 281-286, 2009.
9. Gelorme, J. D., Cox, R. J., and Gutierrez, S. A. R., "Photoresist composition and printed circuit boards and packages made therewith," US Patent, No. 4882245, 1989.
10. Lorenz, H., Despont, M., Fahrni, N., LaBianca, N., Renaud, P., and Vettiger, P., "SU-8: A low-cost negative resist for MEMS," Journal of Micromechanics and Microengineering, Vol. 7, No. 3, pp. 121, 1997.
11. Lee, S. P., Kang, H. W., Lee, S. J., Lee, I., Ko, T., and Cho, D. W., "Development of rapid mask fabrication technology for micro-abrasive jet machining," Journal of Mechanical Science and Technology, Vol. 22, No. 11, pp. 2190-2196, 2008.
12. Saragih, A. S. and Ko, T. J., "A thick SU-8 mask for microabrasive jet machining on glass," The International Journal of Advanced Manufacturing Technology, Vol. 41, No. 7-8, pp. 734-740, 2009.

13. Chan-Park, M.B., Zhang, J., Yan, Y., and Yue, C. Y., "Fabrication of large SU-8 mold with high aspect ratio microchannels by UV exposure dose reduction," Sensors and Actuators B: Chemical, Vol. 101, No. 1-2, pp. 175-182, 2004.

14. Sun, C., Fang, N., Wu, D. M., and Zhang, X., "Projection micro-stereolithography using digital micro-mirror dynamic mask," Sensors and Actuators A: Physical, Vol. 121, No. 1, pp. 113-120, 2005.

15. Choi, J. W., Wicker, R. B., Cho, S. H., Ha, C. S., and Lee, S. H., "Cure depth control for complex 3D microstructure fabrication in dynamic mask projection microstereolithography," Rapid Prototyping J, Vol. 15, No. 1, pp. 59-70, 2009.

16. Kim, H. C., Lee, I. H., and Ko, T. J., "Direct 3D mask modeling for nonplanar workpieces in microabrasive jet machining," The International Journal of Advanced Manufacturing Technology, Vol. 58, No. 1-4, pp. 175-186, 2012.

17. Byiringiro, J. B., Ko, T. J., Kim, H. C. and Lee, I. H., "Fabrication of the photo-resist mask onto 3D non-planar wafer for micro abrasive jet machining," Proc. of the 2012 Mechanical Engineering Conference on Sustainable Research and Innovation, Vol. 4, pp. 155-156, 2012.

18. Kim, H. C., Lee, I. H., and Ko, T. J., "3D tool path generation for micro-abrasive jet machining on 3D curved surface," Int. J. Precis. Eng. Manuf., Vol. 14, No. 9, pp. 1519-1525, 2013.

19. Ferreira, S. L. C., Bruns, R. E., Ferreira, H. S., Matos, G. D., David, J. M., Brandão, G. C., da Silva, E. G. P., Portugal, L. A., dos Reis, P. S., Souza, A. S., and dos Santos, W. N. L., "Box-behnken design: An alternative for the optimization of analytical methods," Analytica Chimica Acta, Vol. 597, No. 2, pp. 179-186, 2007.